

Invariance Learning in Deep Neural Networks with Differentiable Laplace Approximations

Alexander Immer^{*1,2} Tycho F.A. van der Ouderaa^{*3} Vincent Fortuin¹ Gunnar Rätsch^{1,2} Mark van der Wilk³

Abstract

Data augmentation is commonly applied to improve performance of deep learning by enforcing the knowledge that certain transformations on the input preserve the output. Currently, the correct data augmentation is chosen by human effort and costly cross-validation, which makes it cumbersome to apply to new datasets. We develop a convenient gradient-based method for selecting the data augmentation. Our approach relies on phrasing data augmentation as an invariance in the prior distribution and learning it using Bayesian model selection, which has been shown to work in Gaussian processes, but not yet for deep neural networks. We use a differentiable Kronecker-factored Laplace approximation to the marginal likelihood as our objective, which can be optimised without human supervision or validation data. We show that our method can successfully recover invariances present in the data, and that this improves generalisation on image datasets.

1. Introduction

Data augmentation is a commonly used machine learning technique that is essential to high-performing deep learning and computer vision systems. It aims to obtain a model that is *invariant* to a set or distribution of transformations, by fitting a model with inputs that are transformed in a way that is known to leave the output class unchanged. This procedure can be regarded as artificially creating more data, and is well known to increase generalization performance. Yet, choosing the right transformations is an expensive and task-specific process that relies on domain knowledge and human effort, as well as trial-and-error through cross-validation. This quickly becomes cumbersome when many parameters are considered, particularly if they are continuous.

^{*}Equal contribution, order decided by coin flip. ¹Department of Computer Science, ETH Zurich, Switzerland ²Max Planck ETH Center for Learning Systems (CLS) ³Department of Computing, Imperial College London, UK. Correspondence to: Alexander Immer <alexander.immer@inf.ethz.ch>, Tycho F.A. van der Ouderaa <tycho.vanderouderaa@imperial.ac.uk>.

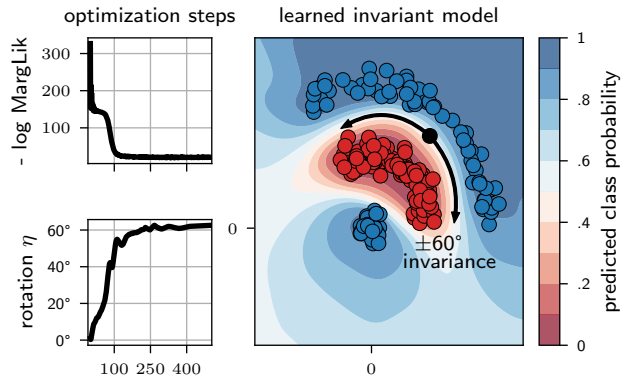


Figure 1. Optimizing the rotational invariance of a neural network by minimizing the Laplace approximation to the log marginal likelihood. The method recovers the true invariance with which the data was generated, during training, without supervision.

We aim to make selecting suitable transformations easier, by learning them by gradient descent together with the neural network weights. Our approach is based on that of [Van der Wilk et al. \(2018\)](#), which casts learning invariances and data augmentations as a Bayesian model selection problem. This view suggests selecting invariances by maximising the *marginal likelihood* by gradient-based optimisation. While this approach was successful in Gaussian process models, it has not yet been demonstrated in deep neural networks, where the marginal likelihood is harder to approximate.

To circumvent this problem, we use the scalable Laplace approximation to the marginal likelihood developed by [Immer et al. \(2021a\)](#), who recently showed that maximising it could successfully select neural network hyperparameters. We extend the method to enable gradient-based optimization of hyperparameters that control invariances. We specify invariances as a distribution on perturbations of the network’s inputs, similar to data augmentation. Samples are taken from the distribution and the model output is averaged. We derive a marginal likelihood approximation for invariant models, and show how to efficiently compute its gradients with respect to the invariance parameters.

We show that the objective successfully selects symmetrical invariance in a toy classification problem and demonstrate differentiable learning of affine invariances on various versions of MNIST, FashionMNIST and CIFAR-10. The invari-

ances that are selected are dataset-specific, indicating that the data is adjusting the invariance, rather than human input. Thus, we can use the objective to differentially learn useful affine invariances in a single training procedure, without the need for cross-validation or human supervision.

2. Related Work

Incorporating symmetries in machine learning models results in faster convergence and higher overall performance, provided that the problem has the relevant symmetries. The convolutional neural network (CNN) (LeCun et al., 1998) is an archetypal example and enforces an equivariance constraint to the group of translations: an inductive bias that has proven useful in many applications. Extensions to other groups allow for equivariance to continuous roto-translations (Worrall et al., 2017; Weiler et al., 2018; Kondor et al., 2018), discrete roto-translations (Cohen & Welling, 2016; Bekkers et al., 2018), scale (Worrall & Welling, 2019), and perturbations (Zaheer et al., 2017), among others. Incorporation of such symmetries has proven to be useful in geometric domains outside of image classification, such as spheres (Cohen et al., 2018) and graphs (Brandstetter et al., 2021), and are applied to a broad class of applications, including molecular dynamics (Batzner et al., 2021) and reinforcement learning (van der Pol et al., 2020). Nevertheless, all of the above rely on knowing the relevant symmetries for a particular problem beforehand. In this work, on the other hand, we aim to automatically learn the correct type and amount of invariance from data through differentiation.

Learning invariance parameters is more challenging than normal weights, as constraining the network to be invariant does not improve the training loss. To circumvent this issue, some methods estimate gradients of a loss on a separate validation set. AutoAugment (Cubuk et al., 2018) learns data augmentation distributions in an outer loop with policy gradients of the validation loss of child models that are trained for many epochs. Lorraine et al. (2020) use the implicit function theorem to compute gradients on the validation loss directly, which allows them to learn data augmentation policies parameterised by another neural network with many parameters. Zhou et al. (2020) use the additional information provided by multiple tasks (meta-learning), and choose an equivariance that gives low validation loss over all tasks.

Reliance on validation sets introduces complexity into the training procedure, particularly if an outer loop is needed. Benton et al. (2020) aim to reduce this reliance by adding an explicit regularisation term to the training loss that encourages diverse data augmentation distributions. While this results in a simple method, validation data may still be needed to tune the regularisation strength in some settings.

Our approach follows previous work that has cast invariance

learning as a Bayesian model selection problem, which (in principle) offers training methods that **1**) do not require training multiple models in inner loops, and **2**) do not rely on separate validation data. Van der Wilk et al. (2018) argued that data augmentation should be expressed as an assumption in the prior, and that this could be done from the point of view of constraining functions in the prior to be invariant. In Gaussian process models, this then allowed a prior with appropriate invariance properties to be selected by maximising the *marginal likelihood* with gradient-based optimisation, without the need for a validation set.

A straightforward extension to neural networks is challenging since the marginal likelihood is more difficult to approximate. Schwöbel et al. (2022) followed a deep kernel learning (Calandra et al., 2016; Wilson et al., 2016) approach, which simplifies the problem by only considering inference in the last layer. While this was successful in simple settings, known limitations of last layer approaches (Ober et al., 2021; van Amersfoort et al., 2021) were exacerbated and caused failure in more complex datasets.

In the context of Bayesian neural networks, data augmentation conflicts with the likelihood and achieving good performance often requires to overcount the data, a trick commonly used in Bayesian deep learning (Zhang et al., 2018; Osawa et al., 2019). Nabarro et al. (2021) instead propose to constrain functions with the augmentation distribution like van der Wilk et al. (2018), but to address the cold-posterior effect (Wenzel et al., 2020; Fortuin et al., 2021). Our work uses the same formulation of the likelihood and additionally enables learning the parameters of the data augmentation.

We rely on recent methods for approximating the marginal likelihood over *all* weights. In particular, a recent Laplace-style approximation by Immer et al. (2021a) that was shown to allow gradient-based optimisation to find hyperparameters, e.g., variances of weight priors and likelihoods. Learning augmentation or invariance parameters is significantly more complex, for which we provide solutions in this work. Laplace approximations have recently seen of surge interest in Bayesian approaches to deep learning (Ritter et al., 2018; Daxberger et al., 2021), in particular due to efficient, yet expressive, Hessian approximations like KFAC (Martens & Grosse, 2015; Botev et al., 2017). Learning invariance parameters relies on such structured approximation because diagonal approximations are insufficient.

Parameterising the invariances we can learn is a crucial element. We follow van der Wilk et al. (2018) and Benton et al. (2020) in expressing invariances as data augmentation distributions which perturb the input in a controllable way, and can be sampled from using the reparameterisation trick. Other approaches that directly control neural connectivity (Zhou et al., 2020; Neyshabur, 2020; van der Ouderaa & van der Wilk, 2021) are interesting in the longer term.

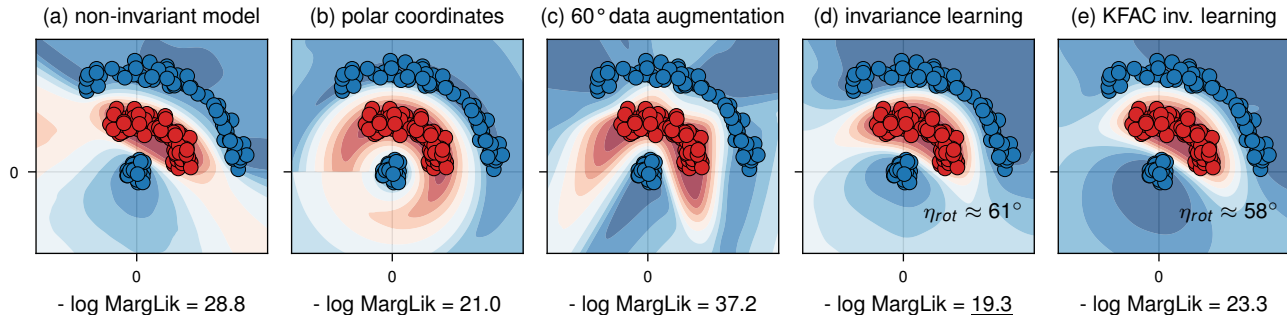


Figure 2. Different approaches to (approximately) invariant neural networks compared to a non-invariant one (a) and their corresponding Laplace log marginal likelihoods. (b): data representation in polar coordinates leads to a good marginal likelihood but requires prior knowledge. (c): standard data augmentation conflicts with the Bayesian model and achieves worse marginal likelihood. (d): treating the invariance or data augmentation parameter as part of a Bayesian model and optimizing it allows to obtain the best marginal likelihood. (e): our efficient approximation based on an augmented KFAC Laplace approximation performs almost as well as the full Gauss-Newton in (d).

3. Background

We consider a supervised learning task with data set $\mathcal{D} = \{(\mathbf{x}_n, \mathbf{y}_n)\}_{n=1}^N$ consisting of N inputs $\mathbf{x} \in \mathbb{R}^D$ and targets $\mathbf{y} \in \mathbb{R}^C$. Our goal is to learn the function $\mathbf{f} : \mathbb{R}^D \rightarrow \mathbb{R}^C$ that relates the inputs and outputs, which we represent as a neural network $\mathbf{f}(\mathbf{x}, \boldsymbol{\theta})$ with parameters $\boldsymbol{\theta}$. We control which solutions for \mathbf{f} are preferred over others (i.e., the *inductive bias*) with hyperparameters \mathcal{H} . Invariance is a particularly helpful inductive bias that constrains the output of \mathbf{f} to remain similar for certain transformations of the input \mathbf{x} . Our goal is to determine what invariance to use together with the network weights.

Invariance specifies a preference for functions which are more constrained. This improves generalisation by allowing a single datapoint to inform predictions for a wider range of inputs. However, selecting the right invariances is hard because they do not necessarily improve the fit to the training data when compared to an unconstrained function \mathbf{f} .

Currently, inductive biases are selected with cross-validation, which trains models with different inductive biases, and selects those with good performance on a validation set (trial-and-error). Bayesian model selection provides a convenient alternative, which allows gradient-based optimisation and does not require separate validation data.

3.1. Bayesian Model Selection

Bayesian inference is a helpful guide for developing inference procedures, as it prescribes how unknowns should be determined from data. A Bayesian inference suggests considering the posterior over all unknowns (MacKay, 2003), weights $\boldsymbol{\theta}$ and hyperparameters \mathcal{H} :

$$p(\boldsymbol{\theta}, \mathcal{H}|\mathcal{D}) = p(\boldsymbol{\theta}|\mathcal{D}, \mathcal{H}) p(\mathcal{H}|\mathcal{D}) \quad (1)$$

$$= \frac{p(\mathcal{D}|\boldsymbol{\theta})p(\boldsymbol{\theta}|\mathcal{H})}{p(\mathcal{D}|\mathcal{H})} \frac{p(\mathcal{D}|\mathcal{H})p(\mathcal{H})}{p(\mathcal{D})}. \quad (2)$$

We observe that the joint posterior decomposes into separate weight and hyperparameter posteriors. We also note that when computing the posterior over the weights for a specific value of hyperparameters $p(\boldsymbol{\theta}|\mathcal{D}, \mathcal{H})$, we compute the $p(\mathcal{D}|\mathcal{H})$, which acts as the likelihood for the posterior over the hyperparameters $p(\mathcal{H}|\mathcal{D})$.

Since computing posteriors is often hard, Bayesian model selection proposes a simplified procedure that only computes the posterior over the weights $p(\boldsymbol{\theta}|\mathcal{D}, \mathcal{H})$. To find the hyperparameters \mathcal{H} , $p(\mathcal{H})$ is assumed to be relatively uniform, and the full posterior is replaced by a point estimate:

$$\mathcal{H}^* = \arg \max_{\mathcal{H}} \log p(\mathcal{D}|\mathcal{H}), \quad (3)$$

which maximises the *marginal likelihood* $p(\mathcal{D}|\mathcal{H})$ that is computed as part of the weight posterior $p(\boldsymbol{\theta}|\mathcal{D}, \mathcal{H})$. This procedure is known as type II maximum likelihood (ML-II) to distinguish it from maximising the usual likelihood $p(\mathcal{D}|\boldsymbol{\theta}, \mathcal{H})$ that also depends on the parameters (ML-I).

ML-II is routinely used in Gaussian processes (Rasmussen & Williams, 2006, §5.2), and trades off model simplicity with the goodness-of-fit (Rasmussen & Ghahramani, 2001). There are also strong relations to quantities from other statistical frameworks, like cross-validation (Fong & Holmes, 2020), Minimum Description Length (Grünwald, 2007), and generalisation error bounds (Germain et al., 2016). Van der Wilk et al. (2018) showed its usefulness for selecting invariances, and elaborated on the mechanism by which it works. The main advantage of the marginal likelihood,

$$p(\mathcal{D}|\mathcal{H}) = \int \prod_{n=1}^N p(\mathbf{y}_n|\mathbf{f}(\mathbf{x}_n, \boldsymbol{\theta}), \mathcal{H}) p(\boldsymbol{\theta}|\mathcal{H}) d\boldsymbol{\theta}, \quad (4)$$

$= p(\mathcal{D}|\boldsymbol{\theta}, \mathcal{H})$

is that it can be computed from the training data alone and optimised with gradients.

3.2. Model Selection for Neural Networks

Computing the marginal likelihood for neural networks involves intractable integrals. The Laplace approximation

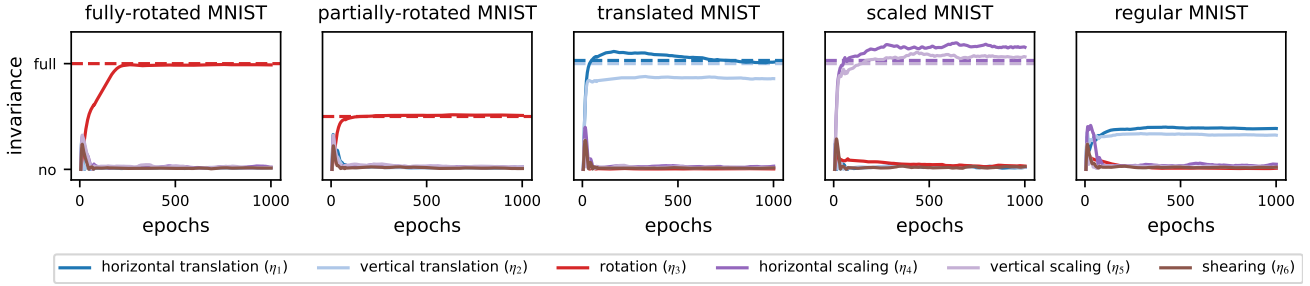


Figure 3. Trajectories of invariance parameters $\boldsymbol{\eta} = [\eta_1, \eta_2, \dots, \eta_6]^T$ over training epochs when trained on different versions of the MNIST dataset. The model automatically learns the correct type and amount of invariance dependent on the observed training data.

(Laplace, 1774; MacKay, 2003, ch. 27) offers a solution, by approximating the posterior $p(\boldsymbol{\theta}|\mathcal{D}, \mathcal{H})$ by a Gaussian $q(\boldsymbol{\theta}) = \mathcal{N}(\boldsymbol{\theta}; \boldsymbol{\mu}, \bar{\mathbf{H}}_{\boldsymbol{\theta}_*})$ with a matched mode and Hessian. Since the posterior is proportional to the joint we obtain

$$\boldsymbol{\mu} = \arg \max_{\boldsymbol{\theta}} \log p(\mathcal{D}, \boldsymbol{\theta}|\mathcal{H}), \quad (5)$$

$$\bar{\mathbf{H}}_{\boldsymbol{\theta}_*} \stackrel{\text{def}}{=} -\nabla_{\boldsymbol{\theta}}^2 \log p(\mathcal{D}, \boldsymbol{\theta}|\mathcal{H})|_{\boldsymbol{\theta}=\boldsymbol{\theta}_*}. \quad (6)$$

The marginal likelihood is the normalising constant, which can consequently be approximated by

$$\log p(\mathcal{D}|\mathcal{H}) \approx \log p(\mathcal{D}, \boldsymbol{\theta}_*|\mathcal{H}) - \frac{1}{2} \log \left| \frac{1}{2\pi} \bar{\mathbf{H}}_{\boldsymbol{\theta}_*} \right|. \quad (7)$$

The joint is computed from the regularised log likelihood:

$$\log p(\mathcal{D}, \boldsymbol{\theta}|\mathcal{H}) = \sum_n \log p(\mathbf{y}_n|\mathbf{x}_n, \boldsymbol{\theta}, \mathcal{H}) + \log p(\boldsymbol{\theta}|\mathcal{H}).$$

Overall, this approach allows us to estimate the marginal likelihood using a classical MAP estimate of the weights, and the local curvature $\bar{\mathbf{H}}_{\boldsymbol{\theta}_*}$. MacKay (1992a;b) first demonstrated this idea on (by today’s standards, small) neural networks. Nowadays, the Hessian of the log likelihood term $\mathbf{H}_{\boldsymbol{\theta}_*} \stackrel{\text{def}}{=} \bar{\mathbf{H}}_{\boldsymbol{\theta}_*} - \nabla_{\boldsymbol{\theta}}^2 \log p(\boldsymbol{\theta}|\mathcal{H})|_{\boldsymbol{\theta}=\boldsymbol{\theta}_*}$ is too large to compute directly, due to it having $\mathcal{O}(P^2)$ non-zero entries in the number of parameters P .

Variational inference also provides an approximation to the marginal likelihood (the ELBO) and has been applied to deep networks. So far, optimising hyperparameters using the ELBO has not seen much success, and early work noted that it hurt performance (Blundell et al., 2015).

3.3. Modern Laplace Approximations

To apply the Laplace approximation in modern neural networks, the high cost of dealing with the full Hessian must be circumvented. Recently, Immer et al. (2021a) proposed using the generalized Gauss-Newton (GGN) and Fisher approximations of the Hessian, and demonstrated successful hyperparameter selection in deep learning models. Further, they do not restrict the Laplace approximation to be at a

mode, which allows for interleaved gradient-based optimization of parameters and hyperparameters during training.

With the Jacobian matrix $\mathbf{J}_{\boldsymbol{\theta}}(\mathbf{x}) \in \mathbb{R}^{C \times P}$ of the network output w.r.t. parameters, and Hessians of the log likelihood w.r.t. network outputs $\boldsymbol{\Lambda}(\mathbf{f}) \stackrel{\text{def}}{=} -\nabla_{\mathbf{f}}^2 \log p(\mathbf{y}|\mathbf{f})$, the GGN simplifies the log-likelihood-dependent term of the Hessian:

$$\mathbf{H}_{\boldsymbol{\theta}} \approx \mathbf{H}_{\boldsymbol{\theta}}^{\text{GGN}} \stackrel{\text{def}}{=} \sum_{n=1}^N \mathbf{J}_{\boldsymbol{\theta}}(\mathbf{x}_n)^\top \boldsymbol{\Lambda}(\mathbf{f}(\mathbf{x}_n; \boldsymbol{\theta})) \mathbf{J}_{\boldsymbol{\theta}}(\mathbf{x}_n). \quad (8)$$

Here, we assume that \mathbf{f} forms the natural parameters of an exponential family likelihood function (Murphy, 2012). In this case, the GGN is optimal in the sense that $\boldsymbol{\Lambda}(\mathbf{f})$ is positive semidefinite while much of the second-order information of the log likelihood is captured (Martens, 2020; Kunstner et al., 2019; Immer et al., 2021b). For example in classification, this means that \mathbf{f} are the logits *before* the softmax. We refer to the resulting approximations as Laplace-GGN. To overcome the still intractable quadratic size in P or NC , Immer et al. (2021a) use structured approximations like KFAC (Martens & Grosse, 2015; Botev et al., 2017). Although in some situations even diagonal approximations work to an extent, they do compromise accuracy, which was also observed by (MacKay, 1992a).

Kronecker-factored approximations to the Gauss-Newton, such as KFAC, are commonly used for Laplace approximations as they provide a better trade-off between performance and complexity (Ritter et al., 2018; Daxberger et al., 2021). KFAC is a block-diagonal approximation to the Gauss-Newton matrix $\mathbf{H}_{\boldsymbol{\theta}}^{\text{GGN}}$ where each block corresponds to a layer in the neural network (Martens & Grosse, 2015; Botev et al., 2017). Further, it is efficient because it represents each block in terms of two Kronecker factors instead of a dense matrix. For example, the GGN block of a layer with $D \times G$ parameters, e.g. a fully-connected layer connecting D to G neurons, would have quadratic memory complexity $\mathcal{O}(D^2G^2)$ while the corresponding Kronecker approximation of KFAC is in $\mathcal{O}(D^2 + G^2)$ and is therefore even tractable for deep neural networks.

Mathematically, KFAC approximates the GGN of the l th block of the neural network parameters by forcing a Kro-

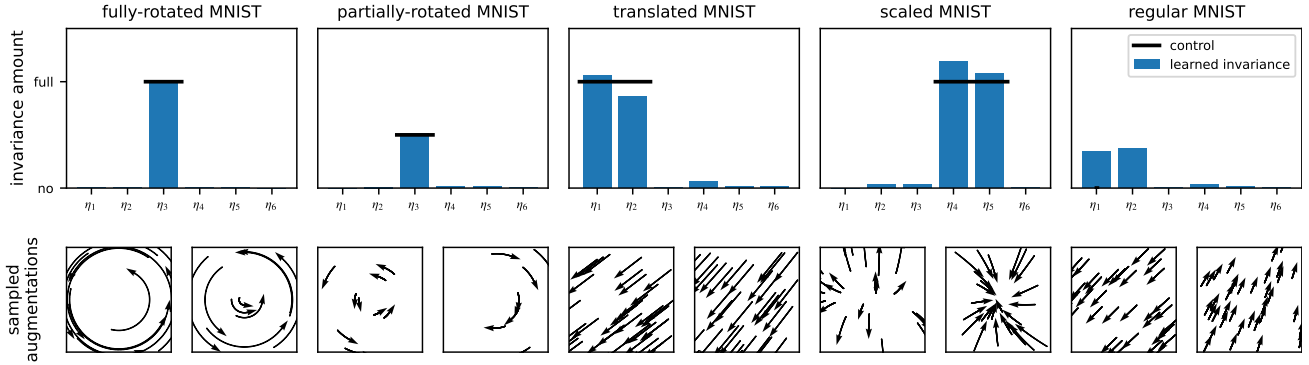


Figure 4. Learned distribution over invariance parameters η after training corresponding to horizontal translation (η_1), vertical translation (η_2), rotation (η_3), horizontal scaling (η_4), vertical scaling (η_5) and shearing (η_6). A control line shows the augmentation added to the datasets. From each distribution, two sampled transformations are represented as flow field. Our model automatically learns the correct type and amount of invariance dependent on the observed training data.

necker factorisation across data points. This would only be exact for a single data point \mathbf{x}_n for which we can write the GGN block corresponding to the parameters of the l th layer as $\mathbf{H}_{l,n}^{\text{GGN}}$ and simplify to a Kronecker product

$$\mathbf{H}_{l,n}^{\text{GGN}} = [\mathbf{a}_{l-1,n} \otimes \mathbf{g}_{l,n}] \mathbf{\Lambda}_n [\mathbf{a}_{l-1,n} \otimes \mathbf{g}_{l,n}]^T \quad (9)$$

$$= [\mathbf{a}_{l-1,n} \mathbf{a}_{l-1,n}^T] \otimes [\mathbf{g}_{l,n} \mathbf{\Lambda}_n \mathbf{g}_{l,n}^T] \quad (10)$$

where $\mathbf{a}_{l-1,n} \in \mathbb{R}^D$ is the input to the l th layer for data point \mathbf{x}_n , $\mathbf{g}_{l,n} \in \mathbb{R}^{G \times C}$ is the transposed Jacobian of the network output with respect to the output of the l th layer for \mathbf{x}_n , and $\mathbf{\Lambda}_n = \mathbf{\Lambda}(\mathbf{f}(\mathbf{x}_n, \boldsymbol{\theta}))$. Thus, the factors in Eq. 9 are the Jacobian terms as in the GGN (Eq. 8) but only for the l th layer. KFAC then approximates the sum over n data points by summing up the Kronecker factors individually instead of breaking the Kronecker-factored structure:

$$\begin{aligned} \mathbf{H}_l^{\text{GGN}} &= \sum_{n=1}^N [\mathbf{a}_{l-1,n} \mathbf{a}_{l-1,n}^T] \otimes [\mathbf{g}_{l,n} \mathbf{\Lambda}_n \mathbf{g}_{l,n}^T] \\ &\approx \frac{1}{N} \left[\sum_{n=1}^N \mathbf{a}_{l-1,n} \mathbf{a}_{l-1,n}^T \right] \otimes \left[\sum_{n=1}^N \mathbf{g}_{l,n} \mathbf{\Lambda}_n \mathbf{g}_{l,n}^T \right] \\ &\stackrel{\text{def}}{=} \frac{1}{N} \mathbf{A}_{l-1} \otimes \mathbf{G}_l, \end{aligned} \quad (11)$$

where $\mathbf{A}_{l-1} \in \mathbb{R}^{D \times D}$ can be understood as the uncentered covariance of the inputs to the l th layer, $\mathbf{a}_{l-1,n}$, and $\mathbf{G}_l \in \mathbb{R}^{G \times G}$ as the uncentered covariance of the $G \times C$ dimensional Jacobians $\mathbf{g}_{l,n}$ over all n .

3.4. Parameterizing Invariance

To perform Bayesian model selection over invariances, we construct functions that are constrained to be invariant, and parameterise the possible invariances. We consider a local invariance that intuitively requires the function to not change “too much” in response to transformed inputs. To obtain an invariant function $\hat{\mathbf{f}}$, we average an unconstrained function \mathbf{f} over the perturbation distribution $p(\mathbf{x}'|\mathbf{x}, \boldsymbol{\eta})$ as used in (van der Wilk et al., 2018):

$$\hat{\mathbf{f}}(\mathbf{x}, \boldsymbol{\theta}, \boldsymbol{\eta}) = \mathbb{E}_{p(\mathbf{x}'|\mathbf{x}, \boldsymbol{\eta})} [\mathbf{f}(\mathbf{x}', \boldsymbol{\theta})], \quad (12)$$

where $\boldsymbol{\eta}$ are parameters that control the perturbation distribution, and therefore the invariance, similar to data augmentation. When the perturbation distribution is uniform on the orbit of a group, we recover exact invariance in $\hat{\mathbf{f}}$ (Kondor, 2008; Ginsbourger et al., 2016).

This procedure can equivalently be seen as modifying the prior on functions (which is implied by the prior on weights) (van der Wilk et al., 2018) or as a modification to the likelihood (Nabarro et al., 2021). In either case, the marginal likelihood will now also depend on $\boldsymbol{\eta}$ because it influences the likelihood function $p(\mathbf{y}|\hat{\mathbf{f}}(\mathbf{x}, \boldsymbol{\theta}, \boldsymbol{\eta}), \mathcal{H})$. Therefore, we also need to apply the augmentation at test time. In the following, we refer to $\hat{\mathbf{f}}$ as **augmented** or **invariant neural network**.

As in previous works, we sample with reparameterisation

$$\mathbf{x}' = \mathbf{g}(\mathbf{x}, \boldsymbol{\epsilon}; \boldsymbol{\eta}) \text{ with } \boldsymbol{\epsilon} \sim p(\boldsymbol{\epsilon}) \quad (13)$$

to generate samples according to $p(\mathbf{x}'|\mathbf{x}, \boldsymbol{\eta})$. Van der Wilk et al. (2018) and Benton et al. (2020) both compute their training objectives using samples generated in this way, and can differentiate with respect to $\boldsymbol{\eta}$ if \mathbf{g} is differentiable. Evaluations of the density $p(\mathbf{x}'|\mathbf{x}, \boldsymbol{\eta})$ are not needed.

The proposed method is general in the sense that it describes how invariances can be learned in arbitrary domains or group structures, given that we can parameterize a suitable data augmentation distribution $p(\mathbf{x}'|\mathbf{x}, \boldsymbol{\eta})$. What parameterization works best in practice remains a research question. In our experiments, we consider a combination of uniform distributions and corresponding parameters $\boldsymbol{\eta} \in \mathbb{R}^6$ over 6 generator matrices that define a probability density over the group of affine transformations, similar to Benton et al. (2020) and detailed in App. A. Note that $p(\mathbf{x}'|\mathbf{x}, \boldsymbol{\eta})$ resembles a data augmentation distribution that can be optimized with respect to $\boldsymbol{\eta}$.

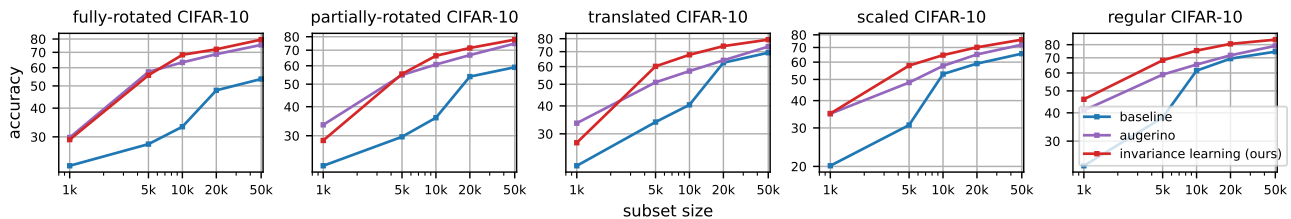


Figure 5. Comparison of test accuracy between baseline, Augerino and our proposed invariance learning model using a ResNet architecture on different versions of the CIFAR-10 dataset, demonstrating improved test accuracy when invariances are learned.

4. Method

We use a Laplace approximation to the marginal likelihood to differentially learn invariance hyperparameters during neural network training, without the use of validation data. In our approach, we integrate the parameterized distribution over invariances (Eq. 13) into a Bayesian neural network model and consider them as hyperparameters. This allows us to approximate the log marginal likelihood that depends on the invariance parameter η using a Laplace-GGN approximation (Sec. 4.1) and optimize it by gradient ascent

$$\eta \leftarrow \eta + \nabla_{\eta} \log p(\mathcal{D}|\eta, \mathcal{M}), \quad (14)$$

in parallel to optimizing neural network parameters (Immer et al., 2021a). We consider η as hyperparameter, i.e., part of \mathcal{H} , but will from now on list them separately as $\mathcal{H} = \mathcal{M} \cup \{\eta\}$ to distinguish the marginal likelihood of an invariant model, $p(\mathcal{D}|\mathcal{M}, \eta)$, from that of an unconstrained model, $p(\mathcal{D}|\mathcal{M})$. \mathcal{M} thus contains only scale hyperparameters like the prior and likelihood precision, which allow simple gradient computation.

In addition to the approach by Immer et al. (2021a), who only optimize scale parameters during training, we need to compute gradients with respect to invariance parameters. While scale parameters only act linearly on the GGN approximation, invariance parameters act non-linearly on it, which leads to difficulties in gradient estimation. Therefore, we provide an efficient method to compute gradients of invariance parameters and non-linear hyperparameters in Sec. 4.3. Further, we extend KFAC to invariant neural networks in Sec. 4.2, which is required for performant approximations to the log marginal likelihood using Laplace’s method.

4.1. Laplace-GGN for an Invariant Model

To optimize the invariance parameters of the neural network $\hat{\mathbf{f}}$, we approximate its log marginal likelihood with a Laplace-GGN approximation,

$$\log p(\mathcal{D}|\eta, \mathcal{M}) \approx \sum_{i=1}^N \log p(\mathbf{y}_n|\hat{\mathbf{f}}(\mathbf{x}_n, \theta, \eta), \mathcal{M}) + \log p(\theta_*|\mathcal{M}) - \frac{1}{2} \log |\hat{\mathbf{H}}_{\theta_*}^{\text{GGN}}|, \quad (15)$$

where the first term is the training loss of $\hat{\mathbf{f}}$ and $\hat{\mathbf{H}}_{\theta_*}^{\text{GGN}}$ is the Gauss-Newton approximation to the Hessian that depends

on η through $\hat{\mathbf{f}}$. We approximate the first term using a finite number of augmentation samples \mathbf{x}' . With S Monte Carlo samples $\epsilon_{1,\dots,S} \sim p(\epsilon)$, we have

$$\hat{\mathbf{f}}(\mathbf{x}, \theta, \eta) \approx \frac{1}{S} \sum_{s=1}^S \mathbf{f}(\mathbf{g}(\mathbf{x}, \epsilon_s; \eta), \theta). \quad (16)$$

Note that we sample ϵ_s independently when computing $\hat{\mathbf{f}}$ for different data points \mathbf{x} during training to avoid correlation. We can similarly define the GGN that depends on η .

The Gauss-Newton approximation to the Hessian for an invariant model requires Jacobians that depend on the augmenting distribution and a log-likelihood Hessian w.r.t the invariant function. The Jacobians of the invariant model are $\hat{\mathbf{J}}_{\theta}(\mathbf{x}, \eta) = \mathbb{E}_{\epsilon}[\mathbf{J}_{\theta}(\mathbf{g}(\mathbf{x}, \epsilon; \eta))]$ and can be approximated using S samples as in Eq. 16. We have the augmented GGN

$$\hat{\mathbf{H}}_{\theta}^{\text{GGN}} \stackrel{\text{def}}{=} \sum_{n=1}^N \hat{\mathbf{J}}_{\theta}(\mathbf{x}_n, \eta)^{\top} \Lambda(\hat{\mathbf{f}}(\mathbf{x}_n, \theta, \eta)) \hat{\mathbf{J}}_{\theta}(\mathbf{x}_n, \eta), \quad (17)$$

where $\Lambda(\hat{\mathbf{f}})$ denotes the Hessian of the log-likelihood function with respect to $\hat{\mathbf{f}}$ as introduced earlier in Eq. 8.

Due to the log-determinant, there is no unbiased stochastic gradient estimate of the Laplace-GGN w.r.t the augmentation parameter η . Thus, we can only optimize η using the gradient ascent updates in Eq. 14 with automatic differentiation tools when full-batch computation is tractable, i.e., with small dataset size N , model size P , and few samples S . This is because computation of the log-determinant scales in the best case as NPS and therefore requires the same amount of memory for automatic differentiation, which would lead to memory issues already for medium-size data sets and neural networks.

To enable invariance learning for deep neural networks, we need to improve scalability in number of parameters P , and data set and sample sizes N and S . Therefore, we first extend Kronecker-factored Laplace approximations to invariant neural networks. Kronecker-factored approximations improve scalability in the number of parameters drastically (cf. Sec. 3). Secondly, we describe a method to efficiently estimate gradients of the Laplace-GGN approximation for large datasets and sample sizes. This method is even relevant outside the scope of this work for optimizing non-linear hyperparameters using the method by Immer et al. (2021a), who only consider parameters linearly affecting the GGN.

Table 1. Marginal Likelihood and Test Accuracy for models using GGN-KFAC on different versions of the MNIST, F-MNIST and CIFAR-10 datasets. Our proposed method outperforms the baselines for almost all models and datasets, in terms of both measures.

Network	Dataset	Model	Marginal Likelihood					Test Accuracy				
			Fully rotated Dataset	Partially rotated Dataset	Translated Dataset	Scaled Dataset	Original Dataset	Fully rotated Dataset	Partially rotated Dataset	Translated Dataset	Scaled Dataset	Original Dataset
MNIST	MLP	Baseline	-31.3k ±99	-23.1k ±29	-36.0k ±10	-17.5k ±28	-10.5k ±5	93.82 ±0.10	95.83 ±0.03	94.15 ±0.02	97.07 ±0.06	98.20 ±0.03
		Augerino	-	-	-	-	-	97.83 ±0.03	96.35 ±0.02	94.47 ±0.08	97.45 ±0.03	98.45 ±0.03
		Learned η (ours)	-9.7k ±25	-10.5k ±27	-14.5k ±11	-11.3k ±22	-6.2k ±33	97.74 ±0.07	97.81 ±0.11	97.28 ±0.05	98.33 ±0.05	98.98 ±0.05
	CNN	Baseline	-14.6k ±1626	-10.7k ±1070	-16.5k ±1014	-9.5k ±225	-5.0k ±428	95.97 ±0.33	97.51 ±0.17	96.54 ±0.29	98.37 ±0.00	99.09 ±0.02
		Augerino	-	-	-	-	-	99.04 ±0.02	98.91 ±0.03	97.79 ±0.09	98.77 ±0.06	98.26 ±0.10
		Learned η (ours)	-6.9k ±77	-7.2k ±295	-8.6k ±136	-7.5k ±54	-4.3k ±27	98.83 ±0.07	98.92 ±0.05	98.69 ±0.07	99.01 ±0.06	99.42 ±0.02
F-MNIST	MLP	Baseline	-55.1k ±117	-46.2k ±184	-52.4k ±36	-39.2k ±27	-25.5k ±6	77.62 ±0.30	81.10 ±0.23	77.68 ±0.10	81.84 ±0.05	88.48 ±0.56
		Augerino	-	-	-	-	-	77.76 ±0.15	81.40 ±0.05	78.05 ±0.10	82.46 ±0.09	89.10 ±0.13
		Learned η (ours)	-29.3k ±63	-29.4k ±148	-36.6k ±17	-34.7k ±201	-22.6k ±42	87.39 ±0.06	86.72 ±0.13	84.62 ±0.08	84.31 ±0.06	89.94 ±0.12
	CNN	Baseline	-58.7k ±189	-49.9k ±275	-53.8k ±257	-43.3k ±488	-28.9k ±165	78.69 ±0.28	82.12 ±0.35	80.33 ±0.19	83.66 ±0.37	89.54 ±0.23
		Augerino	-	-	-	-	-	85.76 ±3.23	81.54 ±0.19	82.94 ±0.13	83.58 ±0.08	90.07 ±0.12
		Learned η (ours)	-26.5k ±101	-27.2k ±0	-29.2k ±65	-30.1k ±0	-21.0k ±233	89.45 ±0.03	88.40 ±0.00	87.73 ±0.20	87.33 ±0.00	91.92 ±0.21
CIFAR-10	ResNet (8-8)	Baseline	-73.1k ±152	-67.5k ±334	-53.7k ±154	-59.3k ±749	-46.5k ±345	51.14 ±0.47	55.29 ±0.70	64.84 ±0.21	59.81 ±0.96	69.74 ±0.75
		Augerino	-	-	-	-	-	70.88 ±0.17	70.95 ±0.26	74.44 ±0.24	70.67 ±0.28	79.34 ±0.36
		Learned η (ours)	-51.1k ±244	-47.8k ±296	-38.6k ±181	-41.7k ±225	-31.2k ±346	71.06 ±0.47	73.03 ±0.45	74.18 ±0.07	71.54 ±0.18	80.22 ±0.24
	ResNet (8-16)	Baseline	-80.9k ±483	-72.8k ±133	-56.2k ±329	-62.0k ±283	-46.1k ±953	54.16 ±0.40	59.90 ±0.12	69.65 ±0.16	66.06 ±0.13	74.13 ±0.51
		Augerino	-	-	-	-	-	75.40 ±0.19	74.76 ±0.34	73.71 ±0.31	72.07 ±0.09	79.03 ±1.04
		Learned η (ours)	-43.1k ±217	-38.7k ±135	-35.4k ±1969	-40.2k ±3404	-30.2k ±2344	79.50 ±0.62	77.71 ±0.46	79.21 ±0.17	76.03 ±0.15	84.19 ±0.76

4.2. Extending KFAC to Invariant Neural Networks

Computing KFAC as described in Sec. 3 for an invariant neural network would not preserve the Kronecker structure and therefore be intractable for deep learning due to the quadratic cost in the numbers of parameters per layer. The Kronecker structure can not be maintained because we have an expectation over augmentation samples \mathbf{x}' on the factors in Eq. 9 that prohibits the simplification to a Kronecker product in Eq. 10.

Similar to KFAC, we enforce the efficient Kronecker-factored structure by approximating the expectation of a Kronecker product as a Kronecker product of expectations. The Jacobians of the l th block of parameters in the invariant model can be expressed as

$$\hat{\mathbf{J}}_{\theta}(\mathbf{x}_n, \boldsymbol{\eta}) = \mathbb{E}_{p(\mathbf{x}'_n | \mathbf{x}_n, \boldsymbol{\eta})}[\mathbf{a}'_{l-1, n} \otimes \mathbf{g}'_{l, n}], \quad (18)$$

where we denote the dependency of the factors on \mathbf{x}' by \mathbf{a}' and \mathbf{g}' . Then, we obtain the KFAC for an invariant model as

$$\begin{aligned} \hat{\mathbf{H}}_{l, n}^{\text{GGN}} &= \mathbb{E}[\mathbf{a}'_{l-1, n} \otimes \mathbf{g}'_{l, n}] \boldsymbol{\Lambda}(\hat{\mathbf{f}}_n) \mathbb{E}[\mathbf{a}'_{l-1, n} \otimes \mathbf{g}'_{l, n}]^T \\ &\approx \mathbb{E}[\mathbf{a}'_{l-1, n}] \mathbb{E}[\mathbf{a}'_{l-1, n}]^T \otimes \mathbb{E}[\mathbf{g}'_{l, n}] \boldsymbol{\Lambda}(\hat{\mathbf{f}}_n) \mathbb{E}[\mathbf{g}'_{l, n}]^T. \end{aligned} \quad (19)$$

To compute the full KFAC, we then sum or average individual Kronecker factors not only over data points but also over augmentation samples to maintain the efficient KFAC structure that scales to large neural networks. Computing and differentiating the log-determinant in Eq. 15 has then cubic complexity in the input and output sizes of the l th layer, D and G , individually, as opposed to cubic complexity in DG . This alleviates the problem with networks that have many parameters P , and enables us to scale marginal likelihood approximations to large invariant models.

4.3. Efficient Gradient Estimation

Naive backpropagation is intractable to compute the gradient of the Laplace approximation with respect to the augmentation parameters $\boldsymbol{\eta}$ because of the log-determinant in

Eq. 15. Computing the log-determinant term requires one pass through the training data because no unbiased stochastic estimate is available. Thus, applying backpropagation on the log-determinant would require a computational graph with space complexity equal to the runtime complexity of estimating the log-determinant which is at least in $\mathcal{O}(NPS)$ and therefore clearly intractable in deep learning settings. In contrast, the log likelihood term of the Laplace approximation can be split up into batches of data points and allows for unbiased stochastic gradients or gradient accumulation.

To enable gradient computation of the log-determinant with respect to augmentation or other non-linear hyperparameters, we can accumulate a *pre-conditioner* and stochastically estimate the other part of the gradient. The partial derivative of the log-determinant in Eq. 15 with respect to an augmentation parameter η_i can be written as

$$\begin{aligned} \frac{\partial}{\partial \eta_i} \log[\hat{\mathbf{H}}] &= \sum_{p, q \in [P]} [\hat{\mathbf{H}}^{-1}]_{p, q} \frac{\partial}{\partial \eta_i} [\hat{\mathbf{H}}]_{p, q} \\ &= \sum_{p, q \in [P]} [\hat{\mathbf{H}}^{-1}]_{p, q} \frac{\partial}{\partial \eta_i} [\sum_{n=1}^N \hat{\mathbf{H}}]_{p, q}, \end{aligned} \quad (20)$$

where $[P]$ refers to the set of all natural numbers from 1 to P . The inverse matrix, $\hat{\mathbf{H}}^{-1}$, which acts as a pre-conditioner of the gradient, requires a full pass through the training data but the second term sums over N data points and can therefore be split up for stochastic or accumulated estimation. Note that for structured GGN approximations like KFAC or diagonal ones, it is not necessary to compute the summands for all (p, q) , e.g., for a diagonal approximation only the terms with $p = q$ are non-zero. Using the above formulation of the gradient, we can first estimate the inverse term and then compute a stochastic estimate of the partial derivative with $M \leq N$ data samples. In conjunction with the KFAC approximation, this enables invariance learning for deep neural networks on large datasets due to improved memory complexity. However, the runtime complexity scales linearly with augmentation samples S .

5. Experiments

5.1. Classification Example

In Fig. 2, we compare our approach using the standard GGN and the KFAC-GGN with three baselines on a classification example that was generated with a soft $\pm 60^\circ$ rotational invariance around the origin. We consider only rotational invariance about the origin with parameter η_{rot} . Our method with both full and KFAC GGN successfully learns the rotational invariance and obtains a similar value for η_{rot} as the data generating process and obtains the best marginal likelihood indicating a better generalisation. For a more detailed illustration, see Fig. 1. The non-invariant model achieves a worse marginal likelihood and standard data augmentation leads to an even lower value due to problems with its likelihood (Nabarro et al., 2021). A model in polar coordinates corresponds to incorporating prior knowledge manually and, as expected, performs on par with our learned model.

5.2. Recovering Known Invariances

To validate whether the model is capable of learning appropriate invariances, we construct datasets that have been augmented by known sets of transformations. We consider a fully-rotated, partially-rotated, scaled, translated, and the original dataset and inspect the invariance parameter vector $\eta = [\eta_1, \eta_2, \dots, \eta_6]^T$ over the training trajectory. In Fig. 3, we show the values of the vector components corresponding to translational, rotational, scale, and shear invariances of an MLP model during training on different versions of MNIST. As reference, a dashed line shows the amount of invariance that we imposed on the datasets. We observe that the model is capable of quickly selecting the correct vector component for each particular problem, as well as the right amount of invariance. On the regular dataset, we find that the model learns translational invariance, which can be explained by translational variation in the dataset itself.

5.3. Invariance Learning in Different Networks

To further assess the effectivity of the method we assess the performance for larger neural networks on a wider range of datasets. We compare our approach in terms of marginal likelihood and test accuracy with a non-invariant baseline and Augerino (Benton et al., 2020). We use MLP and CNN networks on the MNIST (LeCun & Cortes, 2010) and FashionMNIST (Xiao et al., 2017) datasets and ResNet (He et al., 2016) architectures on CIFAR-10 (Krizhevsky et al., 2009). Like Sec. 5.2, we consider fully-rotated, partially-rotated, translated, scaled, and the original versions of these datasets. In the non-invariant model prior parameters are learned using the marginal likelihood (Immer et al., 2021a). For invariance learning, prior parameters and η are jointly learned based on the marginal likelihood. For Augerino, we mini-

mize the regular cross entropy with added regularizing term $-10^{-2}\|\eta\|_2$ and a fixed weight decay of 10^{-4} following Benton et al. (2020). The same parameterization, network architecture and initializations (in particular $\eta = \mathbf{0}$) were used for all methods. All experiments were repeated with three random seeds and reported with the standard error $\frac{\sigma}{\sqrt{3}}$.

The result of this experiment can be found in Table 1. In all cases, we find that our invariance learning method yields better models in terms of marginal likelihood and test accuracy. This holds across the augmented datasets and original datasets. On the original CIFAR-10 dataset we find that learning invariance results in an 8-10 percentage points increase in test accuracy (Tables 1 and 2) compared to the non-invariant baseline.

Table 2. Invariance Learning with KFAC on CIFAR-10 with ResNet (14-16) achieves best test accuracy and marginal likelihood.

ResNet (14-16)	Marginal Likelihood	Test accuracy
Baseline	-40.7 k \pm 268	79.5 \pm 0.26
Augerino	-	83.0 \pm 0.12
Learned η (ours)	-8.4 k \pm 982	88.1 \pm 0.17

5.4. Invariance Learning Improves Data Efficiency

To evaluate the impact of invariance learning on data efficiency, we compare the performance of various models on different subset sizes. In Fig. 5, we show the test accuracy of our model, the non-invariant baseline and Augerino trained on different subsets of MNIST dataset and provide results for all models as well as on F-MNIST and CIFAR-10 in App. E. In general, we find that invariance learning improves performance for all subset sizes. For the rotated, translated, and scaled datasets we see a particularly large gap between the baselines and models where invariance is learned. These findings suggest that learning invariances is generally useful, and particularly in settings where acquiring additional data is costly or only limited data is available.

5.5. On the Learned Distributions

In some instances (see CIFAR-10 results in Apps. C and D), we observed that the model learned translational invariance on the scaled dataset rather than scale invariance. The used independent uniform distributions over invariance components cannot capture correlations between components whereas the scaled dataset was jointly scaled across the horizontal and vertical axes and thus is correlated. We hypothesize that more complex distributions that do allow for capturing correlations could offer a potential solution in such cases, but leave investigation of more complex families to future work.

6. Conclusion

We presented a method that enables automatic invariance learning in deep neural networks directly from training data, without requiring supervision or validation data. The approach uses the marginal likelihood, which is a parameterization-independent quantity coinciding with generalization performance, and differentiable Laplace approximations to allow gradient-based optimization of invariances in deep learning. Experimentally, we verified that the method is capable of learning invariances in MNIST, F-MNIST and CIFAR-10 datasets, leading to better marginal likelihoods and higher test performance. In future work, it would be interesting to consider more complex transformations and apply the method to larger networks.

References

- Batzner, S., Musaelian, A., Sun, L., Geiger, M., Mailoa, J. P., Kornbluth, M., Molinari, N., Smidt, T. E., and Kozinsky, B. Se (3)-equivariant graph neural networks for data-efficient and accurate interatomic potentials. *arXiv preprint arXiv:2101.03164*, 2021.
- Bekkers, E. J., Lafarge, M. W., Veta, M., Eppenhof, K. A., Pluim, J. P., and Duits, R. Roto-translation covariant convolutional networks for medical image analysis. In *International conference on medical image computing and computer-assisted intervention*, pp. 440–448. Springer, 2018.
- Benton, G., Finzi, M., Izmailov, P., and Wilson, A. G. Learning invariances in neural networks. *arXiv preprint arXiv:2010.11882*, 2020.
- Blundell, C., Cornebise, J., Kavukcuoglu, K., and Wierstra, D. Weight uncertainty in neural networks. In *Proceedings of the 32nd International Conference on Machine Learning*, pp. 1613–1622, 2015.
- Botev, A., Ritter, H., and Barber, D. Practical Gauss-Newton optimisation for deep learning. In *International Conference on Machine Learning*, International Convention Centre, Sydney, Australia, 2017. PMLR.
- Brandstetter, J., Hesselink, R., van der Pol, E., Bekkers, E., and Welling, M. Geometric and physical quantities improve e (3) equivariant message passing. *arXiv preprint arXiv:2110.02905*, 2021.
- Calandra, R., Peters, J., Rasmussen, C. E., and Deisenroth, M. P. Manifold gaussian processes for regression. In *2016 International Joint Conference on Neural Networks (IJCNN)*, pp. 3338–3345. IEEE, 2016.
- Cohen, T. and Welling, M. Group equivariant convolutional networks. In *International conference on machine learning*, pp. 2990–2999. PMLR, 2016.
- Cohen, T. S., Geiger, M., Köhler, J., and Welling, M. Spherical cnns. *arXiv preprint arXiv:1801.10130*, 2018.
- Cubuk, E. D., Zoph, B., Mane, D., Vasudevan, V., and Le, Q. V. Autoaugment: Learning augmentation policies from data. *arXiv preprint arXiv:1805.09501*, 2018.
- Daxberger, E., Kristiadi, A., Immer, A., Eschenhagen, R., Bauer, M., and Hennig, P. Laplace redux-effortless bayesian deep learning. *Advances in Neural Information Processing Systems*, 34, 2021.
- Fong, E. and Holmes, C. On the marginal likelihood and cross-validation. *Biometrika*, 107(2):489–496, 2020.
- Fortuin, V., Garriga-Alonso, A., Wenzel, F., Rätsch, G., Turner, R., van der Wilk, M., and Aitchison, L. Bayesian neural network priors revisited. *arXiv preprint arXiv:2102.06571*, 2021.
- Germain, P., Bach, F., Lacoste, A., and Lacoste-Julien, S. Pac-bayesian theory meets bayesian inference. In Lee, D., Sugiyama, M., Luxburg, U., Guyon, I., and Garnett, R. (eds.), *Advances in Neural Information Processing Systems*, volume 29. Curran Associates, Inc., 2016.
- Ginsbourger, D., Roustant, O., and Durrande, N. On degeneracy and invariances of random fields paths with applications in gaussian process modelling. *Journal of Statistical Planning and Inference*, 170:117–128, 2016. ISSN 0378-3758.
- Grünwald, P. D. *The minimum description length principle*. MIT press, 2007.
- He, K., Zhang, X., Ren, S., and Sun, J. Deep residual learning for image recognition. In *2016 IEEE Conference on Computer Vision and Pattern Recognition, CVPR 2016, Las Vegas, NV, USA, June 27-30, 2016*, pp. 770–778. IEEE Computer Society, 2016.
- Immer, A., Bauer, M., Fortuin, V., Rätsch, G., and Khan, M. E. Scalable marginal likelihood estimation for model selection in deep learning. *arXiv preprint arXiv:2104.04975*, 2021a.
- Immer, A., Korzepa, M., and Bauer, M. Improving predictions of bayesian neural nets via local linearization. In *Proceedings of The 24th International Conference on Artificial Intelligence and Statistics*, pp. 703–711, 2021b.
- Jaderberg, M., Simonyan, K., Zisserman, A., et al. Spatial transformer networks. *Advances in neural information processing systems*, 28:2017–2025, 2015.
- Kingma, D. P. and Ba, J. Adam: A method for stochastic optimization. In *International Conference on Learning Representations*, 2015.

- Kingma, D. P. and Welling, M. Auto-encoding variational bayes. *arXiv preprint arXiv:1312.6114*, 2013.
- Kondor, I. R. Group theoretical methods in machine learning, 2008.
- Kondor, R., Lin, Z., and Trivedi, S. Clebsch–gordan nets: a fully fourier space spherical convolutional neural network. *Advances in Neural Information Processing Systems*, 31: 10117–10126, 2018.
- Krizhevsky, A., Hinton, G., et al. Learning multiple layers of features from tiny images. 2009.
- Kunstner, F., Hennig, P., and Balles, L. Limitations of the empirical fisher approximation for natural gradient descent. In *Advances in Neural Information Processing Systems*, pp. 4158–4169, 2019.
- Laplace, P.-S. d. Mémoire sur la probabilité des causes par les événements. *Mémoires de l’Académie royale des sciences de Paris (Savants étrangers)*, 6:621–656, 1774.
- LeCun, Y. and Cortes, C. MNIST handwritten digit database. <http://yann.lecun.com/exdb/mnist/>, 2010. URL <http://yann.lecun.com/exdb/mnist/>.
- LeCun, Y., Bottou, L., Bengio, Y., and Haffner, P. Gradient-based learning applied to document recognition. *Proceedings of the IEEE*, 86(11):2278–2324, 1998.
- Lorraine, J., Vicol, P., and Duvenaud, D. Optimizing millions of hyperparameters by implicit differentiation. In Chiappa, S. and Calandra, R. (eds.), *Proceedings of the Twenty Third International Conference on Artificial Intelligence and Statistics*, volume 108 of *Proceedings of Machine Learning Research*, pp. 1540–1552. PMLR, 26–28 Aug 2020.
- MacKay, D. J. Bayesian model comparison and backprop nets. In *Advances in neural information processing systems*, pp. 839–846, 1992a.
- MacKay, D. J. The evidence framework applied to classification networks. *Neural computation*, 4(5):720–736, 1992b.
- MacKay, D. J. *Information theory, inference and learning algorithms*. Cambridge university press, 2003.
- Martens, J. New insights and perspectives on the natural gradient method. *Journal of Machine Learning Research*, 21(146):1–76, 2020.
- Martens, J. and Grosse, R. Optimizing neural networks with kronecker-factored approximate curvature. In *International conference on machine learning*, pp. 2408–2417, 2015.
- Moler, C. and Van Loan, C. Nineteen dubious ways to compute the exponential of a matrix, twenty-five years later. *SIAM review*, 45(1):3–49, 2003.
- Murphy, K. P. *Machine learning: a probabilistic perspective*. MIT press, 2012.
- Nabarro, S., Ganev, S., Garriga-Alonso, A., Fortuin, V., van der Wilk, M., and Aitchison, L. Data augmentation in bayesian neural networks and the cold posterior effect. *arXiv preprint arXiv:2106.05586*, 2021.
- Neyshabur, B. Towards learning convolutions from scratch. In Larochelle, H., Ranzato, M., Hadsell, R., Balcan, M. F., and Lin, H. (eds.), *Advances in Neural Information Processing Systems*, volume 33, pp. 8078–8088. Curran Associates, Inc., 2020.
- Ober, S. W., Rasmussen, C. E., and van der Wilk, M. The promises and pitfalls of deep kernel learning. In de Campos, C. and Maathuis, M. H. (eds.), *Proceedings of the Thirty-Seventh Conference on Uncertainty in Artificial Intelligence (UAI)*, volume 161 of *Proceedings of Machine Learning Research*, pp. 1206–1216. PMLR, 27–30 Jul 2021.
- Osawa, K., Swaroop, S., Khan, M. E. E., Jain, A., Eschenhagen, R., Turner, R. E., and Yokota, R. Practical deep learning with bayesian principles. In *Advances in Neural Information Processing Systems*, pp. 4289–4301, 2019.
- Rasmussen, C. E. and Ghahramani, Z. Occam’s razor. In *Advances in neural information processing systems*, pp. 294–300, 2001.
- Rasmussen, C. E. and Williams, C. K. *Gaussian processes for machine learning*. MIT press Cambridge, MA, 2006.
- Ritter, H., Botev, A., and Barber, D. A scalable laplace approximation for neural networks. In *International Conference on Learning Representations*, 2018.
- Schwöbel, P., Jørgensen, M., Ober, S. W., and van der Wilk, M. Last layer marginal likelihood for invariance learning. In *Proceedings of the Twenty Fifth International Conference on Artificial Intelligence and Statistics (AISTATS)*, 2022.
- van Amersfoort, J., Smith, L., Jesson, A., Key, O., and Gal, Y. Improving deterministic uncertainty estimation in deep learning for classification and regression. *CoRR*, abs/2102.11409, 2021.
- van der Ouderaa, T. F. and van der Wilk, M. Learning invariant weights in neural networks. In *Workshop in Uncertainty & Robustness in Deep Learning, ICML*, 2021.

- van der Pol, E., Worrall, D., van Hoof, H., Oliehoek, F., and Welling, M. Mdp homomorphic networks: Group symmetries in reinforcement learning. *Advances in Neural Information Processing Systems*, 33, 2020.
- van der Wilk, M., Bauer, M., John, S., and Hensman, J. Learning invariances using the marginal likelihood. In *Advances in Neural Information Processing Systems*, pp. 9938–9948, 2018.
- Weiler, M., Geiger, M., Welling, M., Boomsma, W., and Cohen, T. 3d steerable cnns: Learning rotationally equivariant features in volumetric data. *arXiv preprint arXiv:1807.02547*, 2018.
- Wenzel, F., Roth, K., Veeling, B. S., Światkowski, J., Tran, L., Mandt, S., Snoek, J., Salimans, T., Jenatton, R., and Nowozin, S. How good is the bayes posterior in deep neural networks really? In *International Conference on Machine Learning*, 2020.
- Wilson, A. G., Hu, Z., Salakhutdinov, R., and Xing, E. P. Deep kernel learning. In *Artificial intelligence and statistics*, pp. 370–378, 2016.
- Worrall, D. E. and Welling, M. Deep scale-spaces: Equivariance over scale. *arXiv preprint arXiv:1905.11697*, 2019.
- Worrall, D. E., Garbin, S. J., Turmukhambetov, D., and Brostow, G. J. Harmonic networks: Deep translation and rotation equivariance. In *Proceedings of the IEEE Conference on Computer Vision and Pattern Recognition*, pp. 5028–5037, 2017.
- Xiao, H., Rasul, K., and Vollgraf, R. Fashion-mnist: a novel image dataset for benchmarking machine learning algorithms, 2017.
- Zaheer, M., Kottur, S., Ravanbakhsh, S., Poczos, B., Salakhutdinov, R., and Smola, A. Deep sets. *arXiv preprint arXiv:1703.06114*, 2017.
- Zhang, G., Sun, S., Duvenaud, D., and Grosse, R. Noisy natural gradient as variational inference. In *International Conference on Machine Learning*, pp. 5852–5861, 2018.
- Zhang, H., Dauphin, Y. N., and Ma, T. Fixup initialization: Residual learning without normalization. In *International Conference on Learning Representations*, 2019.
- Zhou, A., Knowles, T., and Finn, C. Meta-learning symmetries by reparameterization. *arXiv preprint arXiv:2007.02933*, 2020.

Appendix: Invariance Learning in Deep Neural Networks with Differentiable Laplace Approximations

A. Affine invariance parameterization

We apply the re-parameterization trick (Kingma & Welling, 2013) to define the augmentation distribution as a learnable probability distribution that is differentiable with respect to the parameters:

$$z \in p(\mathbf{x}'|\mathbf{x}, \boldsymbol{\eta}) \rightarrow z = g_{\boldsymbol{\epsilon}}(\mathbf{x}'|\mathbf{x}, \boldsymbol{\eta}), \quad \boldsymbol{\epsilon} \in U[-1, 1]^k \quad (21)$$

A general affine parameterization (Benton et al., 2020) can be obtained using $k=6$ generator matrices $\mathbf{G}_1, \dots, \mathbf{G}_6$ and learnable parameters $\boldsymbol{\eta} = [\eta_1, \dots, \eta_6]^T$ for respective horizontal translation, vertical translations, rotations, horizontal scaling, vertical scaling, and shearing:

$$\begin{aligned} \mathbf{G}_1 &= \begin{bmatrix} 0 & 0 & 1 \\ 0 & 0 & 0 \\ 0 & 0 & 0 \end{bmatrix}, & \mathbf{G}_2 &= \begin{bmatrix} 0 & 0 & 0 \\ 0 & 0 & 1 \\ 0 & 0 & 0 \end{bmatrix}, & \mathbf{G}_3 &= \begin{bmatrix} 0 & -1 & 0 \\ 1 & 0 & 0 \\ 0 & 0 & 0 \end{bmatrix} \\ \mathbf{G}_4 &= \begin{bmatrix} 1 & 0 & 0 \\ 0 & 0 & 0 \\ 0 & 0 & 0 \end{bmatrix}, & \mathbf{G}_5 &= \begin{bmatrix} 0 & 0 & 0 \\ 0 & 1 & 0 \\ 0 & 0 & 0 \end{bmatrix}, & \mathbf{G}_6 &= \begin{bmatrix} 0 & 1 & 0 \\ 1 & 0 & 0 \\ 0 & 0 & 0 \end{bmatrix} \end{aligned}$$

To calculate $\mathbf{x}'_{(x',y')}$, defined to be the value of \mathbf{x}' corresponding location $(x', y') \in \mathbb{R}^2$ on the 2-dimensional grid, we apply an inverse of the forward transformation matrix to find pixel locations in the original image:

$$\begin{bmatrix} x \\ y \end{bmatrix} = \exp\left(\sum_i \epsilon_i \eta_i \mathbf{G}_i\right)^{-1} \begin{bmatrix} x' \\ y' \end{bmatrix} \quad (22)$$

where $\exp(M) = \sum_{n=0}^{\infty} \frac{1}{n!} M^n$ denotes the matrix exponential (Moler & Van Loan, 2003), and the transformations becomes

$$g_{\boldsymbol{\epsilon}}(\mathbf{x}'_{(x',y')}|\mathbf{x}, \boldsymbol{\eta}) = \mathbf{x}_{(x,y)} \quad (23)$$

where pixel values in the output $\mathbf{x}'_{(x',y')}$ are calculated exactly on the grid, and the locations in the input $\mathbf{x}_{(x,y)}$ are obtained through bilinear sampling, which can be, as all of the other steps, be automatically differentiated (Jaderberg et al., 2015). Furthermore, the entire process is highly efficient as the matrix exponential and inverse are applied on a very small 3x3 matrix and the grid resampling steps are fully parallelizable across all pixels.

B. Training details

B.1. Dataset details

The alternative datasets were created by applying the following transformations to the original datapoints:

Partially rotated dataset: Every sample rotated by radian angle θ , sampled from $\theta \sim U[-\frac{\pi}{2}, \frac{\pi}{2}]$.

Fully rotated dataset: Every sample rotated by radian angle θ , sampled from $\theta \sim U[-\pi, \pi]$.

Translated dataset: Translated samples relatively by dx and dy pixels, sampled from $dx, dy \sim U[-8, 8]$.

Scaled dataset: Every sample scaled around center with $\exp(s)$, sampled from $s \sim U[-\log(2), \log(2)]$.

B.2. Network Architectures

For the MLP we use a single hidden layer with 1000 hidden units and a \tanh activation function. For the CNN experiments we used a convolutional neural network with three convolutional layers with 3×3 filters, 1 stride, 1 padding, bias weights with increasing channels sizes (3-16-32-64) followed by a linear layers with 256 hidden layers with ReLU activation function between layers.

For CIFAR-10, we used ResNets with fixup parameterization and initialization (Zhang et al., 2019) to avoid batch norm, which conflicts with a Bayesian model (Wenzel et al., 2020). The ResNets sizes are indicated by (input-channels, width) in the tables and figures. We use ResNets (8, 8), (8, 16), and (16, 16). Larger networks require more gradient accumulation and are too expensive to run for all subset sizes and data set transformations. However, it is important to note that the ResNets can easily fit the training data to 100% accuracy. Following Immer et al. (2021a), we use prior precision hyperparameters \mathcal{M} per neural network layer and use a learning rate of 0.05.

B.3. Training parameters

For the MNIST and F-MNIST experiments, we trained our models for 1000 epochs with a batch size of 1000 and 31 augmentation samples. The Adam optimizer was used with a learning rate of 0.005 cosine decayed to 0.0001 and a momentum of 0.9 for the network weights, and for the invariance and hyperparameters we used a learning rate of 0.05 together with a 10 epochs burn-in period. Each experiment was repeated 3 times with different random seeds. For the MNIST and F-MNIST subset of data results in App. E, we use the same hyperparameters and 1000 epochs for subset sizes [312, 1250, 5000, 20000].

For the CIFAR-10 experiments we trained the ResNets for 200 epochs on the full data with initial learning rate of 0.1 using SGD with momentum of 0.9 and cosine learning rate decay to 10^{-6} as common for ResNet training. We use a batch size of 250 and accumulate gradients with respect to augmentation parameters for $M = 5000$ data points using $S = 20$ augmentation samples. We optimize η using Adam (Kingma & Ba, 2015) starting from epoch 10 with learning rate 0.005. All results are averaged across 3 seeds. For the additional results in For Augerino (Benton et al., 2020) we use the same learning rate, 0.005 for η and default weight-decay of 10^{-4} as used in their experiments. For the CIFAR-10 subset of data results in App. E, we use the same hyperparameters but [600, 400, 300, 250] epochs for subset sizes [1000, 5000, 10000, 20000], respectively. Each experiment is repeated for three random seeds.

B.4. Classification Example

For the toy classification example with $N = 200$ data points, we use fully-connected neural network with a single hidden layer of 50 neurons and \tanh activation. All methods train with 500 steps with a learning rate of 0.1 using the Adam optimizer (Kingma & Ba, 2015). For the prior precision hyperparameter in \mathcal{M} , we use the same learning rate of 0.1. For the augmentation parameter η , we use a lower learning rate of 0.005 and decay it with cosine-decay to 0.0001 due to the stochasticity of the gradients. For data augmentation and our method, we use $S = 100$ augmentation samples. Each step, we optimize neural network parameters, augmentation parameters η , and scale hyperparameters \mathcal{M} , which is a single prior precision in this case. We plot the improved posterior predictive for Laplace approximations (Immer et al., 2021b) in both Fig. 1 and Fig. 2. The log marginal likelihood values given in Fig. 2 are all computed with a full Laplace-GGN, even for the KFAC variant, for comparability of the estimates. The hyperparameters \mathcal{M} , η in Fig. 2 (e) are optimized using the augmented KFAC method proposed in Sec. 4.

C. Additional results: augmentation trajectories

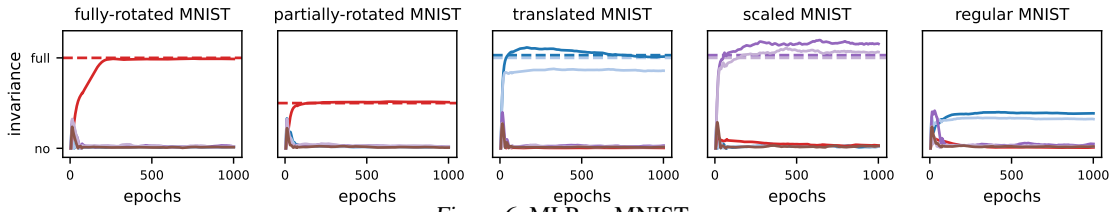


Figure 6. MLP on MNIST

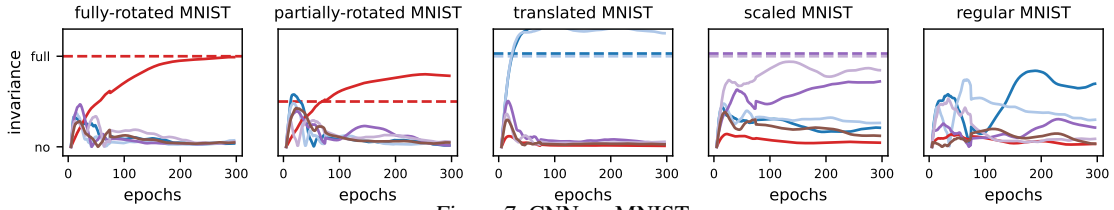


Figure 7. CNN on MNIST

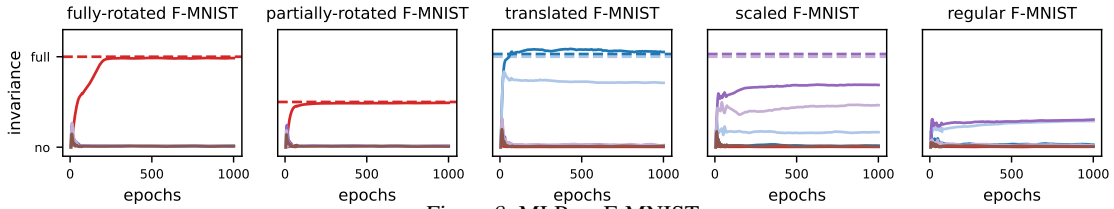


Figure 8. MLP on F-MNIST

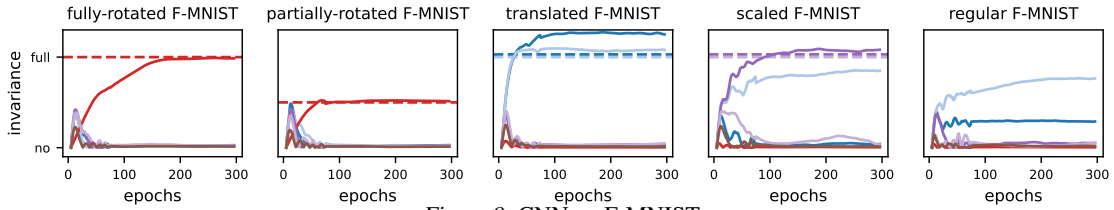


Figure 9. CNN on F-MNIST

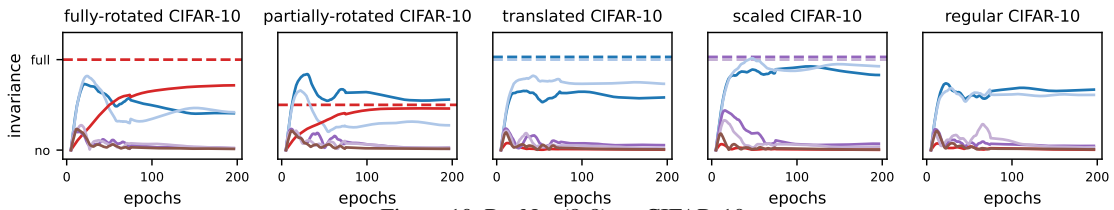


Figure 10. ResNet (8-8) on CIFAR-10

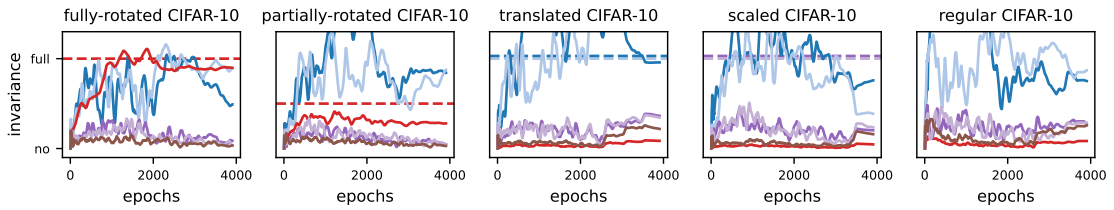
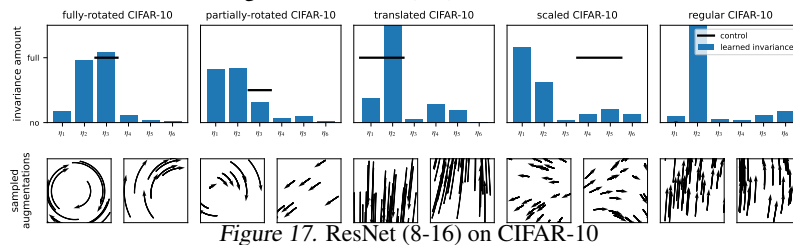
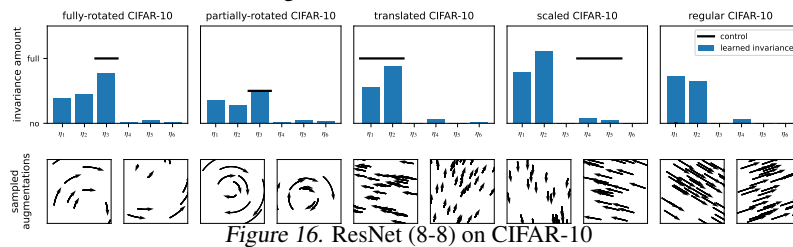
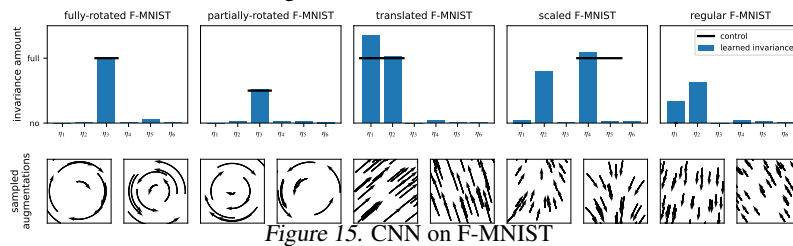
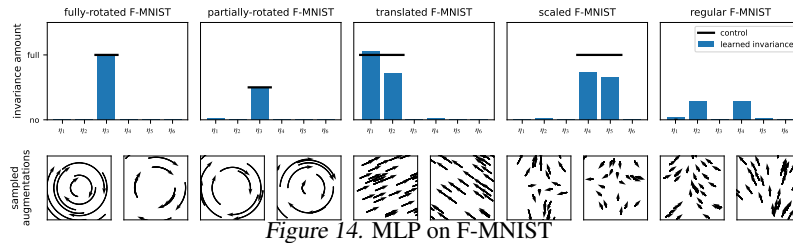
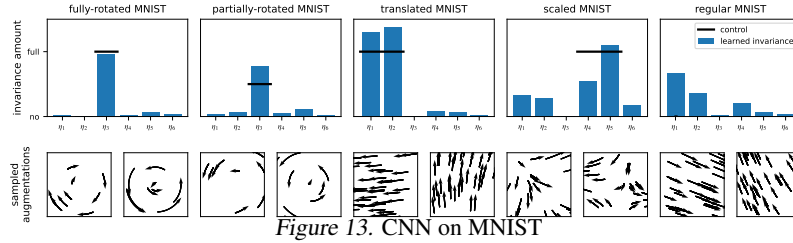
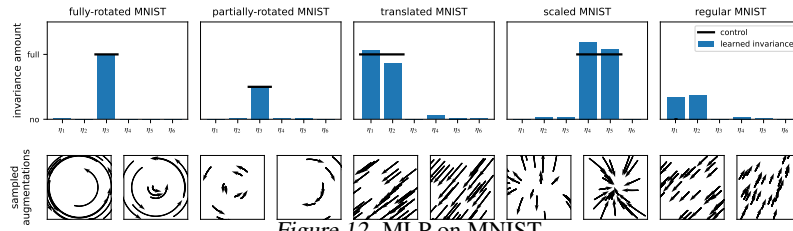


Figure 11. ResNet (8-16) on CIFAR-10 (with biased gradients)

— horizontal translation (η_1) — vertical translation (η_2) — rotation (η_3) — horizontal scaling (η_4) — vertical scaling (η_5) — shearing (η_6)

D. Additional results: learned invariances



E. Additional results: subset experiments

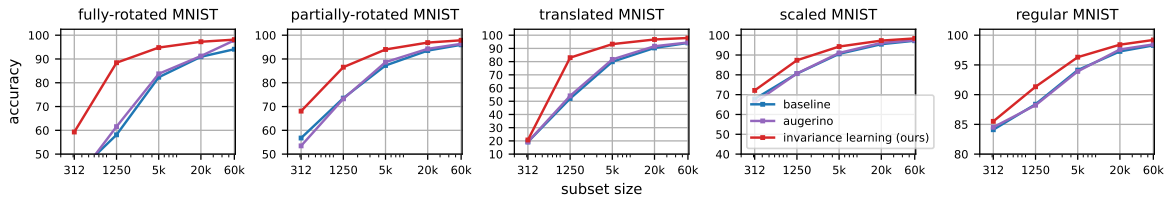


Figure 18. MLP on MNIST

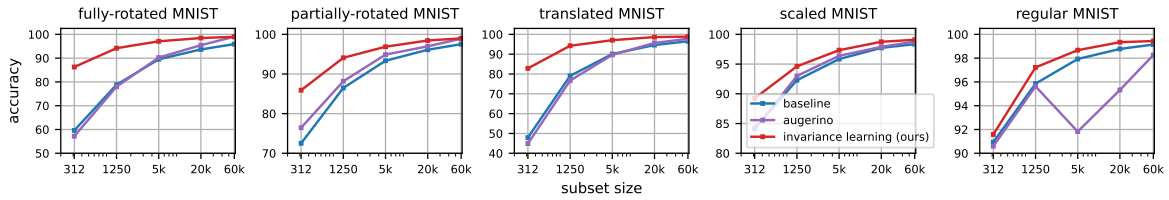


Figure 19. CNN on MNIST

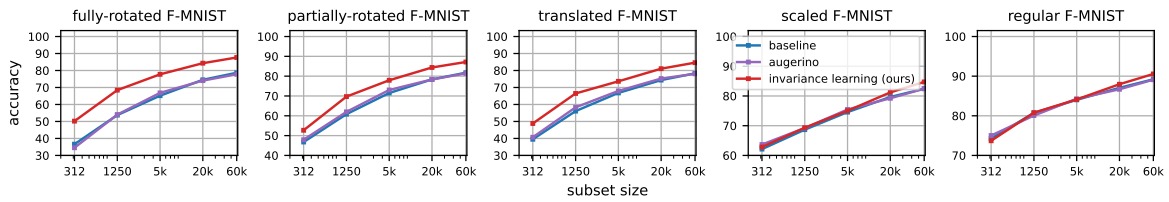


Figure 20. MLP on F-MNIST

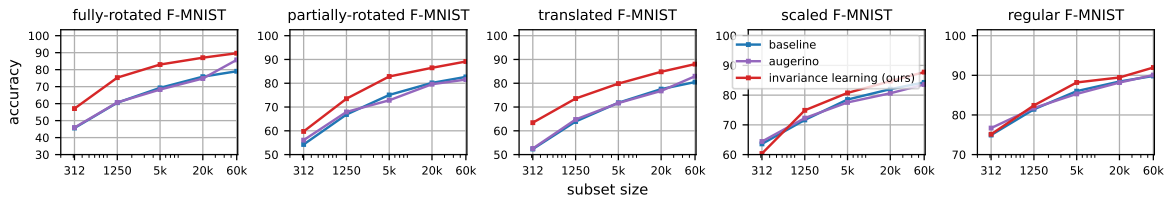


Figure 21. CNN on F-MNIST

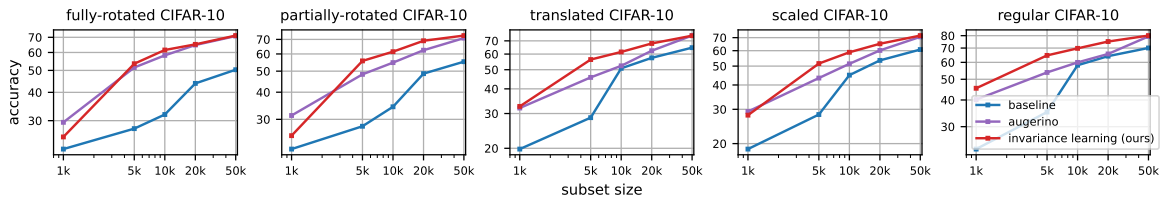


Figure 22. ResNet (8-8) on CIFAR-10

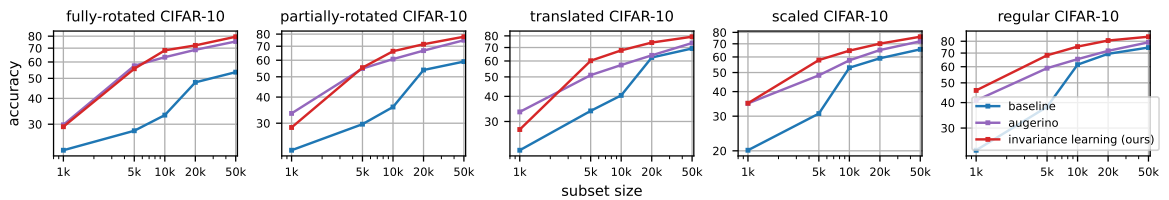


Figure 23. ResNet (8-16) on CIFAR-10